International Journal of Civil Engineering

Structure-Concrete

Finite element modeling of incremental bridge launching and study on behavior of the bridge during construction stages

A. Shojaei[1], H. Tajmir Riahi[2,*], M. Hirmand[3]

Received: January 2014, Accepted: April 2014

Abstract

Incremental launching is a widespread bridge erection technique which may offer many advantages for bridge designers. Since internal forces of deck vary perpetually during construction stages, simulation and modeling of the bridge behavior, for each step of launching, are tedious and time consuming tasks. The problem becomes much more complicated in construction progression. Considering other load cases such as support settlements or temperature effects makes the problem more intricate. Therefore, modeling of construction stages entails a reliable, simple, economical and fast algorithmic solution. In this paper, a new Finite Element (FE) model for study on static behavior of bridges during launching is presented. Also a simple method is introduced to normalize all quantities in the problem. The new FE model eliminates many limitations of some previous models. To exemplify, the present model is capable to simulate all the stages of launching, yet some conventional models of launching are insufficient for them. The problem roots from the main assumptions considered to develop these models. Nevertheless, by using the results of the present FE model, some solutions are presented to improve accuracy of the conventional models for the initial stages. It is shown that first span of the bridge plays a very important role for initial stages; it was eliminated in most researches. Also a new simple model is developed named as "semi infinite beam" model. By using the developed model with a simple optimization approach, some optimal values for launching nose specifications are obtained. The study may be suitable for practical usages and also useful for optimizing the nose-deck system of incrementally launched bridges.

Keywords: *Incremental bridge launching, Finite element method, Nose – deck system, Optimization, Semi infinite beam model.*

1. Introduction

Bridge piers are constructed first in incremental bridge launching method and after that, deck segments are pushed forward above them until they reach their final positions (Fig. 1). Constructing, curing, pre-stressing and pushing the segments are done on a construction platform close to bridge abutments [2, 3]. These segments may be over a half- length of the bridge spans; therefore, number of structural weak points in junctions is reduced considerably. Some other advantages such as high speed working due to eliminating casting molds, reducing manpower and constructional costs, proper and accurate supervisions, no needing to block obstacles under the bridge during launching and minimizing the destruction of the environment in construction location, make incremental launching more competitive in comparison to other erection techniques [4-6]. Temporary tensions occurred during construction stages may be different and much more critical than those in service life.

Therefore, an appropriate method should be used to reduce these forces and thus avoid wasting the advantages of the method by using overdesigned structural members. Different methods have so far been introduced by engineers and researchers for this purpose. Among them, using a nose-deck system, owing to its simplicity and efficiency, has been known as the standard method. In this sense, a light nose girder, attached in front of the deck, is used to reduce the cantilever moment of deck at its end [2]. Nose specifications have significant effects on the nose-deck interaction.

Researchers have focused on two main categories of study for incremental bridge launching. The first category is related to study on the nose-deck interaction, and it pertains to find some proper values for nose specifications. To this end, a simple model of the nose-deck system is required. Marchetti used the elastic load analyze method to present a simplified model for launched bridges [7]. This model became as a prototype model for other researches. For instance, Rosignoli studied on this model to investigate the nose-deck system and find optimal specifications of nose via a try and error method [4]. Also Fontan et al. discussed the optimal ranges of nose specifications by some mathematical optimization approaches via Marchetti's model [8].

** Corresponding author: tajmir@eng.ui.ac.ir*
1 Graduate student of structural engineering, Isfahan University of Technology, Isfahan, Iran
2 Assistant professor, University of Isfahan, Isfahan, Iran
3 Graduate student of structural Engineering, Sharif University of Technology, Tehran, Iran

[DOI: 10.22068/IJCE.13.1.112]

Fig. 1 Incremental bridge launching [1]

The second category is related to developing proper methods for simulating stages of construction during launching. Analyzing movement of a superstructure over fixed piers needs to consider different schemes for arrangement of the piers. Nevertheless, the best method is the fastest one which works with repetitive algorithms and can be easily implemented in computer programming. The method should provide most information in the least possible time. Rosignoli simulated the incremental bridge launching with Reduced Transfer Matrix (RTM) method [9]. Sasmal et al. presented Transient Transfer Matrix (TTM) method for structural analysis of launched bridges [10]. Sasmal and Ramanjaneyulu developed this method for pre-stressed concrete bridges [11]. Arici and Granata extended the TTM method to study construction stages of curved box girder bridges with constant radius [12]. RTM and TTM methods are generally inefficient for parametric study of nose-deck interaction. Therefore, majority of the researchers have shown their results only for some case studies.

The present study uses finite element method to model incremental launching for both aforementioned categories. It will be shown that not only does this method have the advantages of the RTM and TTM methods but also it is much more systematic and convenient for computer programming. Also a simple method is used to normalize all the parameters involved in the model. An extensive study is done along with considering some new factors such as shear strain and temperature gradient effects; they were eliminated in some previous studies. It will be shown that studying on the rotation of deck sections leads the analyzer to evaluate the accuracy of Marchetti's model easily. Therefore, some solutions are suggested to improve the accuracy of this conventional model for initial stages of launching as well as forthcoming ones. The effects of first span length and platform of the construction, on the structural behavior of the bridge, are included. Some solutions are suggested to optimize the bridge performance by taking these two factors in to account. Likewise, a new simplified model is developed named as "semi-infinite beam" model. The model is useful for parametric studies on the nose-deck interaction. In the final analysis, a simple mathematical approach is investigated to find some proper ranges for optimal design of the nose girders.

2. Assumptions and Definitions of the Parameters

In this study some assumptions are considered for generating the finite element model. This section gives some explanations about assumptions and definitions used here.

2. 1. Arrangement scheme of piers

Various schemes of pier arrangement can be considered in the model. But it is more reasonable to set the arrangement of piers based on optimum static performance of the bridge in service time. Constructional stresses can be controlled by other practices such as using a light nose girder attached in front of deck, pre-stressing or using some temporary piers. In the present study, the bridge structure consists of some identical mid spans and shorter end ones. Most bridges with continuous system were constructed according to this pattern around the world due to its structural and architectural benefits.

2. 2. Definition of stage, station and phase

The nose tip passes through all spans during launching and the number of launching spans equals the launching stage. The number of piers behind the launching stage is defined as the station. For each stage of launching two different phases can be considered. Phase one refers to the position that nose tip has not reached the next pier and the nose-deck system has a cantilever scheme. This phase lasts till nose tip reaches the next pier. Phase two starts after that and lasts till nose girder passes the pier completely. Definitions of stage, station and phase are shown in Fig. 2.

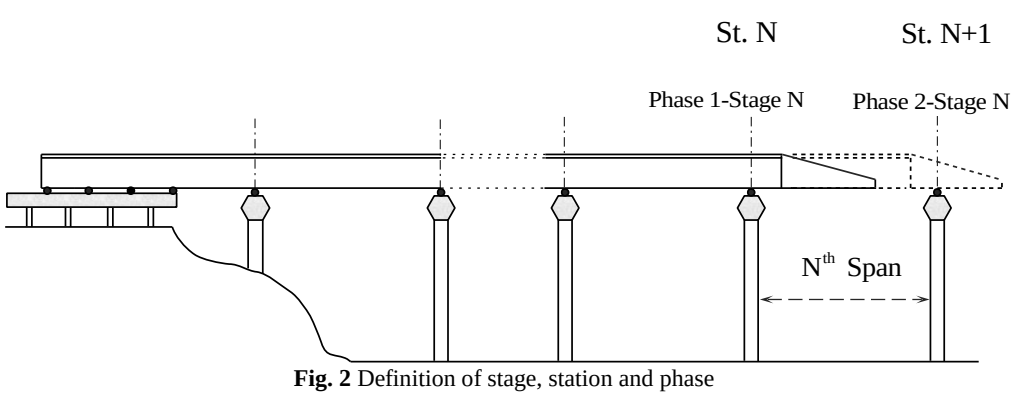

Fig. 2 Definition of stage, station and phase

[DOI: 10.22068/IJCE.13.1.112]

2. 3. Specifications of launching nose

Although majority of noses are constructed with tapered sections, in this study it is assumed that the nose girder is prismatic. Using mean values of the tapered nose specifications for an equivalent prismatic nose will introduce a very small error (less than 2%) [13, 14]; therefore, this assumption is accurate enough. Flexural stiffness, dead load, length and height of nose are defined by E_nI_n, q_n, L_n and H_n, respectively.

2. 4. Normalizing the formulations

In this study, three main specifications of deck including flexural stiffness (E_DI_D), dead load (q_D) and mid spans length (L_D) have been considered as the measurement scales i.e. their values are assumed to be unit. Any other quantity in the problem can be stated normalized to these values. Therefore, L_n, q_n, E_nI_n and H_n, in normalized dimensionless formats, are presented by four dimensionless parameters as β_L (ratio of nose length to mid span length), β_q (ratio of nose load to deck load), β_{EI} (ratio of nose flexural stiffness to deck flexural stiffness) and β_{HN} (ratio of nose section height to mid span length). Such an approach leads to expressing the unknown forces in a dimensionless format as a coefficient of deck characteristics. For instance, internal moment for each section of deck is obtained as a coefficient of $q_DL_D^2$. Length of end spans and deck height, in the normalized format, are denoted by β_1 and β_{HD}, respectively. This method is so beneficiary and useful for parametric studies on the nose-deck interaction.

2. 5. Deck specifications

It is assumed that the bridge is straight and without any horizontal curvilinear. In most cases, especially for highway bridges, adoption of box girders is usual. Since box girders have high torsional rigidity, the torsional moment effect is not critical for these bridges during launching. Therefore, the straight beam theory can be sufficient [9]. It is also assumed that the mechanical specifications of deck including flexural rigidity and dead load are constant along its length.

Since all the deck sections periodically experience negative and positive moments during launching, it is reasonable to use a central prestressing scheme. This central prestressing will not affect bending moment of deck; hence the launching internal forces can be calculated irrespective to this prestressing. In practice, after the launching time, this central prestressing will be replaced with an appropriate parabolic pre-stressing scheme.

Pre-stressed composite bridges may experience considerable deformations due to shear slip of the shear studs located between concrete slab and steel girders [2, 15, 16]. However, the effect of shear slip is not considered and only shear strain effect is considered here.

2. 6. Modeling the construction platform

During launching, one or two deck segments are kept on the construction platform usually. When nose reaches piers, axial stiffness of platform can be neglected in comparison to very high axial stiffness of the bridge piers. Therefore, platform segments have a cantilever behavior during lunching, and the effects of segments on the platform can be replaced with a concentrated shear force and a moment on the first station. The average normalized length of segments on the platform is denoted by β_0.

3. Finite Element Formulation

It is well-understood that the axial stiffness of the bridge deck is high and its axial force is relatively small; therefore, axial displacements are negligible and thus usual beam elements are sufficient to model the continuous deck of the bridge; for these elements axial degree of freedom is not considered.

In this section, bold letters refer to matrix variables. For a beam element, shown in Fig. 3, nodal forces vector, **r**, and displacements vector, **d**, for a generic element are defined as follow:

$$\mathbf{r} = \langle \mathbf{r}_i \quad \mathbf{r}_j \rangle^T ; \mathbf{r}_i = \langle r_1 \quad r_2 \rangle^T , \mathbf{r}_j = \langle r_3 \quad r_4 \rangle^T \tag{1}$$

$$\mathbf{d} = \langle \mathbf{d}_i \quad \mathbf{d}_j \rangle^T ; \mathbf{d}_i = \langle d_1 \quad d_2 \rangle^T , \mathbf{d}_j = \langle d_3 \quad d_4 \rangle^T \tag{2}$$

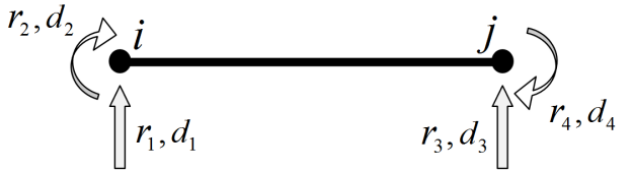

Fig. 3 The Beam element

The finite element formulation for a beam element, in the view of stiffness method, can be written as:

$$\mathbf{r} - \mathbf{r}_f = \mathbf{k}.\mathbf{d} \quad , \quad \mathbf{r}_f = \mathbf{r}_q + \mathbf{r}_t \tag{3}$$

where $\mathbf{k}$ is the element stiffness matrix and $\mathbf{r}_f$ is summation of $\mathbf{r}_q$ (equivalent element nodal forces vector due to external distributed loads) and $\mathbf{r}_t$ (equivalent element nodal forces vector due to thermal loads). The element stiffness matrix, by assuming all the properties to be constant along the element, is as follows:

[DOI: 10.22068/IJCE.13.1.112]

$$\mathbf{k} = \begin{bmatrix} \mathbf{s}_{ii} & \mathbf{s}_{ij} \\ \mathbf{s}_{ji} & \mathbf{s}_{jj} \end{bmatrix} \tag{4}$$

where:

$$\mathbf{s}_{ii} = \mu \begin{bmatrix} \frac{12}{L} & 6 \\ 6 & \frac{4\left(L^2 + 3EI\frac{\tau}{GA}\right)}{L} \end{bmatrix},\ \mathbf{s}_{ij} = \mu \begin{bmatrix} -\frac{12}{L} & 6 \\ -6 & \frac{2\left(L^2 - 6EI\frac{\tau}{GA}\right)}{L} \end{bmatrix},\ \mathbf{s}_{ji} = \mu \begin{bmatrix} -\frac{12}{L} & -6 \\ 6 & \frac{2\left(L^2 - 6EI\frac{\tau}{GA}\right)}{L} \end{bmatrix},\ \mathbf{s}_{jj} = \mu \begin{bmatrix} \frac{12}{L} & -6 \\ -6 & \frac{4\left(L^2 + 3EI\frac{\tau}{GA}\right)}{L} \end{bmatrix} \tag{5}$$

$$\mu = \frac{EI}{L^2 + 12EI\frac{\tau}{GA}} \tag{6}$$

E and G are the modulus of elasticity and the shear modulus of the material, I and A are the moment of inertia and area of the section, L is the length of the element and τ is the shear constant (ratio of the maximum shear stress to the average shear stress at the section). Considering a uniform distributed load on the element and a linear thermal gradient within the element section, $\mathbf{r}_q$ and $\mathbf{r}_t$ vectors can be written as:

$$\mathbf{r}_q = \left\langle \frac{qL}{2} \quad \frac{qL^2}{12} \quad \frac{qL}{2} \quad -\frac{qL^2}{12} \right\rangle^T \tag{7}$$

$$\mathbf{r}_t = \frac{EI.\alpha_T.\Delta T}{H} \langle 0 \quad -1 \quad 0 \quad -1 \rangle^T \tag{8}$$

where, q, ΔT, H and α_T are the uniform distributed load on the element per unit length, the difference between the temperature at top and bottom of the section, height of the section and the thermal expansion coefficient, respectively.

As it was described before, the characteristics of the structure should be written in a dimensionless format by normalizing them on the basis of the deck specifications. Therefore, the values of the parameters in the stiffness matrix and load vectors should be written in a normalized format.

Shear stiffness is only considered for the concrete deck section, and it is neglected for the nose girder. The τ/GA term, which shows the effects of shear deformation in the stiffness matrix, can be written in a normalized dimensionless format as:

$$\frac{\tau}{GA} = \beta_s.\beta_r^2;\ \beta_r = \frac{r_{gyr}}{L_D},\ \beta_s = 2\tau(1+\nu) \tag{9}$$

r_{gyr} and ν are the radius of gyration of the deck section and the Poisson's ratio, respectively. To elucidate, the stiffness matrix of first element (first bridge span), in a parametric form, using equations (4-6), can be written as follows:

To sum up, analysis of the whole structure can be performed by solving the following system of equations:

$$\mathbf{R} - \mathbf{R}_f = \mathbf{K}.\mathbf{D} \tag{11}$$

Where $\mathbf{K}$ is the global stiffness matrix, $\mathbf{R}$ is the global nodal forces vector and $\mathbf{R}_f$ is the global equivalent nodal forces vector obtained by superposition of external distributed loads and thermal loads, and $\mathbf{D}$ is the global nodal displacement vector. Support settlements can be directly taken into account; it suffice to replace their normalized values in the appropriate row of $\mathbf{D}$.

When numbering of the elements is started from the first span of the bridge and continued one by one to the last element, $\mathbf{K}$ and $\mathbf{R}_f$ can be assembled as:

According to equation (12), the global stiffness matrix is obtained banded and the calculation time of solving equation (11) can be reduced significantly due to narrow band width of $\mathbf{K}$. A banded stiffness matrix (which is the result of appropriate element numbering) compensates its higher dimensions in comparison to matrices used in RTM and TTM methods. Moreover, the RTM and TTM methods require repetitive computations and satisfying boundary conditions of each element in each step, while in the FE method boundary conditions are directly imposed and the solution is thoroughly summarized to build the global stiffness matrix and the nodal forces vectors. As a repercussion, the FE method may be more suitable for systematic computer analysis.

[DOI: 10.22068/IJCE.13.1.112]

$$\mathbf{K}^{element\,1} =$$

$$\begin{bmatrix} \frac{12\beta_{EI}}{\beta_1^3+12\beta_1\beta_{EI}\beta_r^2\beta_s} & \frac{6\beta_{EI}}{\beta_1^2+12\beta_1\beta_{EI}\beta_r^2\beta_s} & -\frac{12\beta_{EI}}{\beta_1^3+12\beta_1\beta_{EI}\beta_r^2\beta_s} & \frac{6\beta_{EI}}{\beta_1^2+12\beta_1\beta_{EI}\beta_r^2\beta_s} \\ & \frac{\beta_{EI}}{\beta_1}+\frac{3\beta_1\beta_{EI}}{\beta_1^2+12\beta_1\beta_{EI}\beta_r^2\beta_s} & -\frac{6\beta_{EI}}{\beta_1^2+12\beta_1\beta_{EI}\beta_r^2\beta_s} & -\frac{\beta_{EI}}{\beta_1}+\frac{3\beta_1\beta_{EI}}{\beta_1^2+12\beta_1\beta_{EI}\beta_r^2\beta_s} \\ & & \frac{12\beta_{EI}}{\beta_1^3+12\beta_1\beta_{EI}\beta_r^2\beta_s} & -\frac{6\beta_{EI}}{\beta_1^2+\beta_1\beta_{EI}\beta_r^2\beta_s} \\ \text{SYM} & & & \frac{\beta_{EI}}{\beta_1}+\frac{3\beta_1\beta_{EI}}{\beta_1^2+12\beta_1\beta_{EI}\beta_r^2\beta_s} \end{bmatrix} \tag{10}$$

$$\begin{cases} \mathbf{K}(2a-1:2a,2a-1:2a)=\mathbf{s}_{jj}^{elementa-1}+\mathbf{s}_{ii}^{elementa} \\ \mathbf{K}(2a-3:2a-2,2a-1:2a)=\mathbf{s}_{ij}^{elementa-1} \\ \mathbf{K}(2a-1:2a,2a-3:2a-2)=\mathbf{s}_{ji}^{elementa-1} \\ \mathbf{K}(otherwise)=0 \end{cases} \quad ; \quad \text{For } a=1:\text{number of elements} \tag{12}$$

$$\mathbf{R}_f(2a-1:2a)=\mathbf{r}_{f\,j}^{element\,a-1}+\mathbf{r}_{f\,i}^{element\,a} \tag{13}$$

4. Nose-Deck Interaction

In contrary to simplified conventional model that assumes infinite number of spans behind a station, the present FE model does not have this limitation. Fig. 4 shows moment variation of fifteenth station for different values of β_{EI} with β_L and β_q as 0.5 and 0.1, respectively. This station is selected because it can represent stations with infinite number of spans behind them. Nose end distance from the under study station is denoted by α that is normalized based on the length of mid spans.

According to Fig. 4, in phase 1 (zone A) internal moment of this section is independent of the nose flexural stiffness; therefore, curves are completely overlapped in this region. In contrary to phase 1, in phase 2 (zone B), the moment is dependent on β_{EI} significantly.

Optimum specifications of the nose should be chosen in a manner that the maximum moment of deck in the foremost pier in phases 1 and 2 of launching, denoted by M_1 and M_2 in Fig. 4, approaches to -1/12 as much as possible [8]. Moreover, not any maximum moment should emerge along the deck that exceeds that of M_1 and M_2 (marked with triangles). As shown in Fig. 4, choosing a sufficiently large value for β_{EI} may control the latter criterion. It should be noted that the station moment in zone C (moment of second station before launching span) is also dependent on the nose specifications. An optimal design for nose specifications must prevent the maximum moment of zone C to be more critical than maximum moment of zones A and B. More complexities arise out of optimization of nose specifications due to interdependency of the nose characteristics. Therefore, an exact and effective optimization requires mathematical approaches along with difficult engineering assessments. Fontan et al. completely discussed this problem in a mathematical point of view [8]. However, in Section 7, a brief investigation into optimization of the nose specification via a simple and insightful approach will be presented.

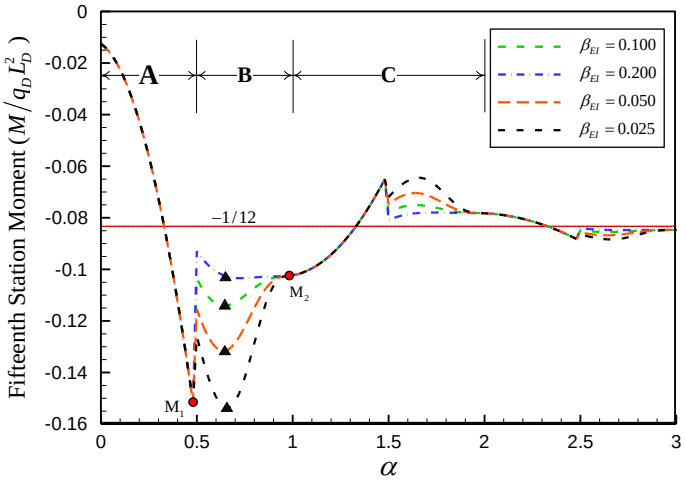

Fig. 4 Moment variation of fifteenth station for β_L=0.5, β_q=0.1 and different values of β_{EI}

[DOI: 10.22068/IJCE.13.1.112]

Fig. 5 shows the variation of fifteenth station moment in fifteenth stage for different values of β_L and constant values of β_{EI} and β_q. Also Fig. 6 shows the variation of this station for different values of β_q and constant values of β_{EI} and β_L. According to these figures, increscent of β_q has an identical effect with decreasing of β_L on performance of the system. It can be concluded that larger values for β_q require larger values for length of the nose girder to achieve the equality of M_1 and M_2 (Fig. 4). Hence, for each value of β_q there is a proper value for β_L which causes this matter. Some compatible values for nose specifications which make its performance approximately optimum during launching are as $\beta_L = 0.65$, $\beta_q = 0.1$ and $\beta_{EI} = 0.2$. It should be remarked here that these values are rather used in practice, and they have been suggested by some of the researchers in the literature [2, 5]. Fig. 7 shows the fifteenth station moment obtained by these well-known values of nose specifications. It should be noted that the yellow mark in the figure indicates the maximum moment of station for fifteenth stage of launching. Hereinafter, these values are considered for nose specifications to study on the effect of other parameters that governs the nose-deck interaction.

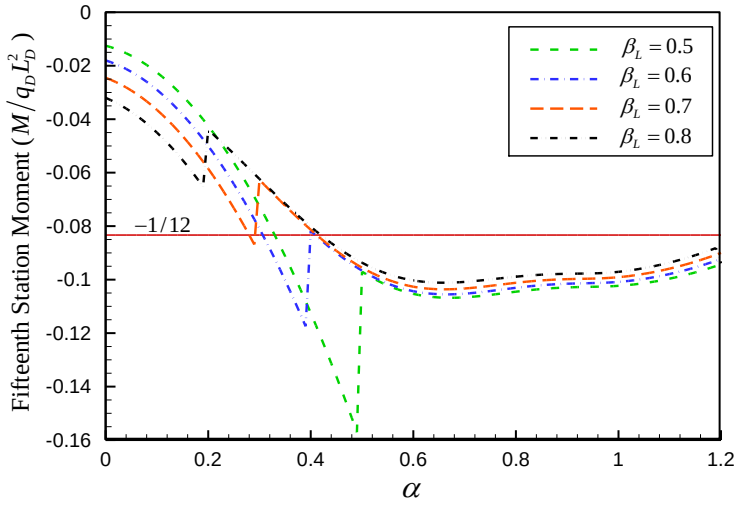

Fig. 5 Variation of fifteenth station moment in fifteenth stage for β_{EI} =0.15, β_q=0.1 and different values of β_L

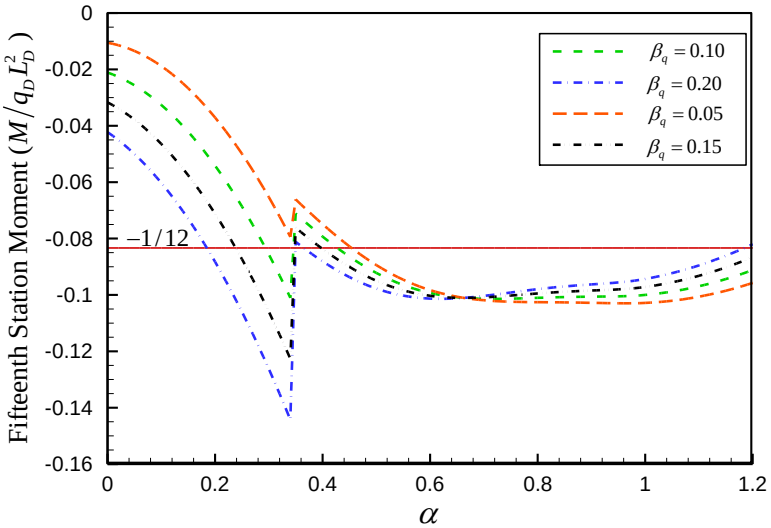

Fig. 6 variation of fifteenth station moment in fifteenth stage for β_{EI} =0.2, β_L=0.65 and different values of β_q

[DOI: 10.22068/IJCE.13.1.112]

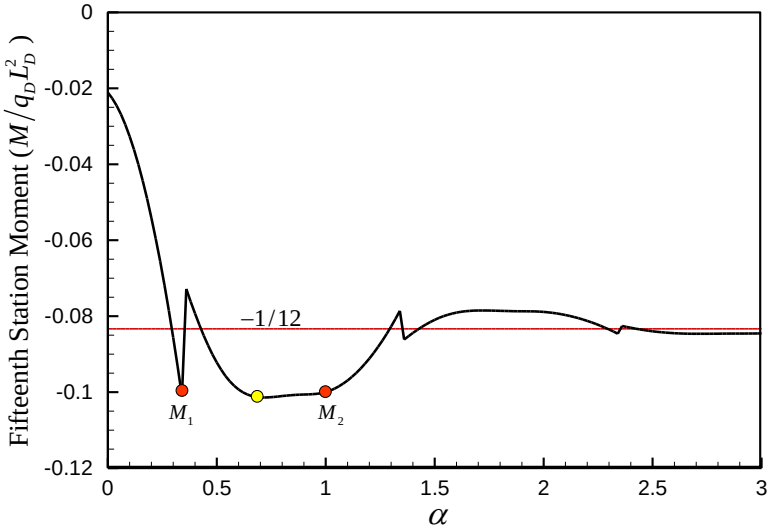

Fig. 7 Variation of fifteenth station moment for optimum nose specifications

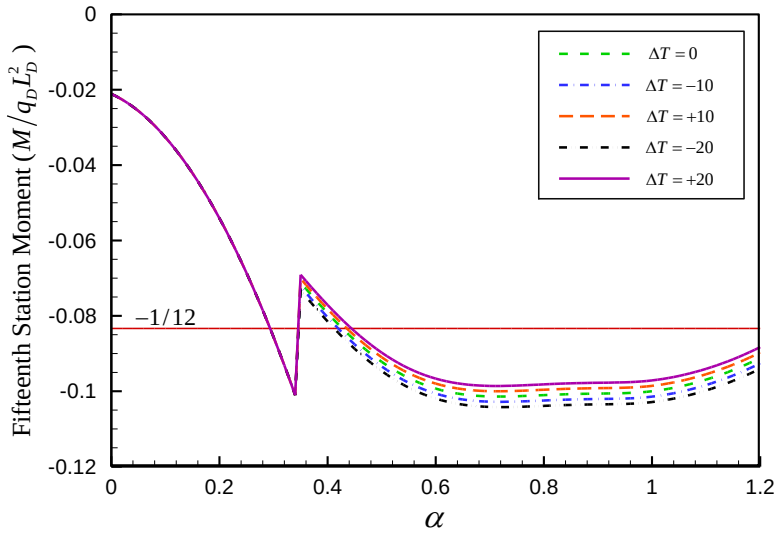

Fig. 8 Variation of fifteenth station moment with different values of temperature gradient

In order to show the temperature gradient effects on performance of the nose-deck system, variation of fifteenth station moment with different values of temperature gradient is illustrated in Fig. 8. β_{HN} and β_{HD} are considered to be 1/20 and 1/10, respectively. The coefficients of thermal expansion for concrete deck and steel nose girder are assumed to be 11.3×10^{-6} 1/C° and 8.5×10^{-6} 1/C°, respectively. This figure indicates that the effect of temperature gradient on variation of station moment is not significant in general. Moreover, it can be concluded that negative gradient (higher temperature in top of the section) increases the station moment and makes the condition more critical. To study on the shear strain deformation effect on the nose-deck interaction, variation of fifteenth station moment regarding this effect is shown in Fig. 9. The moment station variation is plotted once with shear strain effects neglected ($\beta_s = 0$) and once with respect to this effect for $\beta_s = 3.2$ and different values of β_r. According to this figure, it can be concluded, the shear strain effect on the station moment for values of β_r less than 0.02 is negligible. Generally, for composite box girder sections, β_r is less than 0.02 (see [16]) and thus shear strain effect is negligible in most practical cases. It should be noted that in spite of shear strain effect, shear slip effect of studs for composite bridges may be more significant as mentioned before.

[DOI: 10.22068/IJCE.13.1.112]

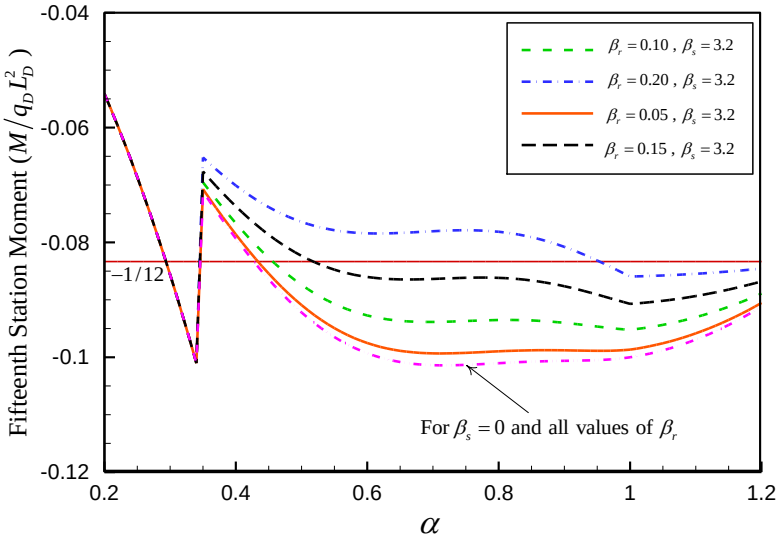

Fig. 9 Variation of fifteenth station moment considering shear strain effect

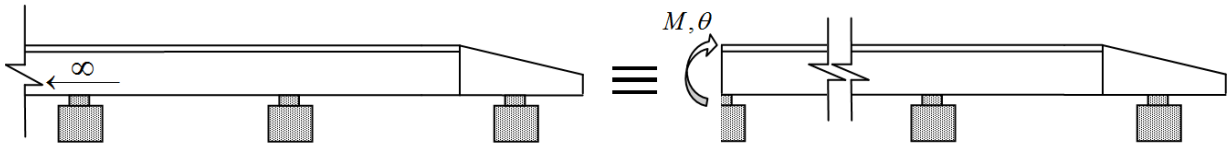

Fig. 10 Assumption of the conventional simplified model

5. Study on the Conventional Simplified Model

As discussed earlier, when there are a large number of spans behind a station, structural behavior of the bridge, at the section of this station, is identical to a continuous beam with infinite number of spans. Fig. 10 shows a continuous deck during launching with infinite spans behind the launching stage. Marchetti proposed the rotation of a generic section θ, for a launching deck with infinite number of spans as follows [7]:

$$\theta = a_1 M + a_2 ;$$
$$a_1 = \frac{1}{2\sqrt{3E_D I_D}} \approx 0.288675 \frac{1}{E_D I_D}, \qquad (14)$$
$$a_2 = \frac{q_D {L_D}^3}{24\sqrt{3E_D I_D}} \approx 0.024056 \frac{q_D {L_D}^3}{E_D I_D}$$

where M is the station moment, a_1 and a_2 are constant coefficients dependant on the deck specifications only. By using this relation for any station of deck, the problem can be reduced to analyze a continuous beam with lower degrees of indeterminacy. In this section, the precision of this formula is examined for each stage of launching to find out when continuous bridge reaches its infinite scheme.

Fig. 11 illustrates the variation of internal moment and rotation of stations 2 to 6. In this figure it is assumed that all spans are identical and β_0 is zero. Also the behavior of fifteenth station is shown in this figure. The superscript (*) implies that the rotation is obtained by equation (14). The results obtained by Marchetti's model are included in the figure.

As shown, stations 2 to 6 may be more critical than farther stations (for example fifteenth station). Accurate rotations of these stations are different from results given by equation (14); especially for stations 2 to 4. But rotation of station 5 has good matching with the results of this equation and fifteenth station behavior. For station 6 and next stations, results obtained from equation (14) completely agree with the results obtained from the FE model. This conclusion is valid for any nose specifications. In a nutshell, (14) is valid only when there are at least 5 spans behind the station.

On the other hand, for fourth station and the next ones when nose tip is 2.5 to 3 spans farther, the station rotation nearly tends to zero and remains constant i.e. treats as a fixed support. So it can be concluded that existence of at least three stations behind and farther a station is required to approximately assume the station as a fixed support. Therefore, instead of analyzing the whole structure, a new simplified model named as "semi infinite beam" model can be analyzed (Fig. 12). It should be noted that this model may not be useful when there are not enough spans (at least 3 spans) behind the fixed support; it is the problem for launching of the initial stages.

[DOI: 10.22068/IJCE.13.1.112]

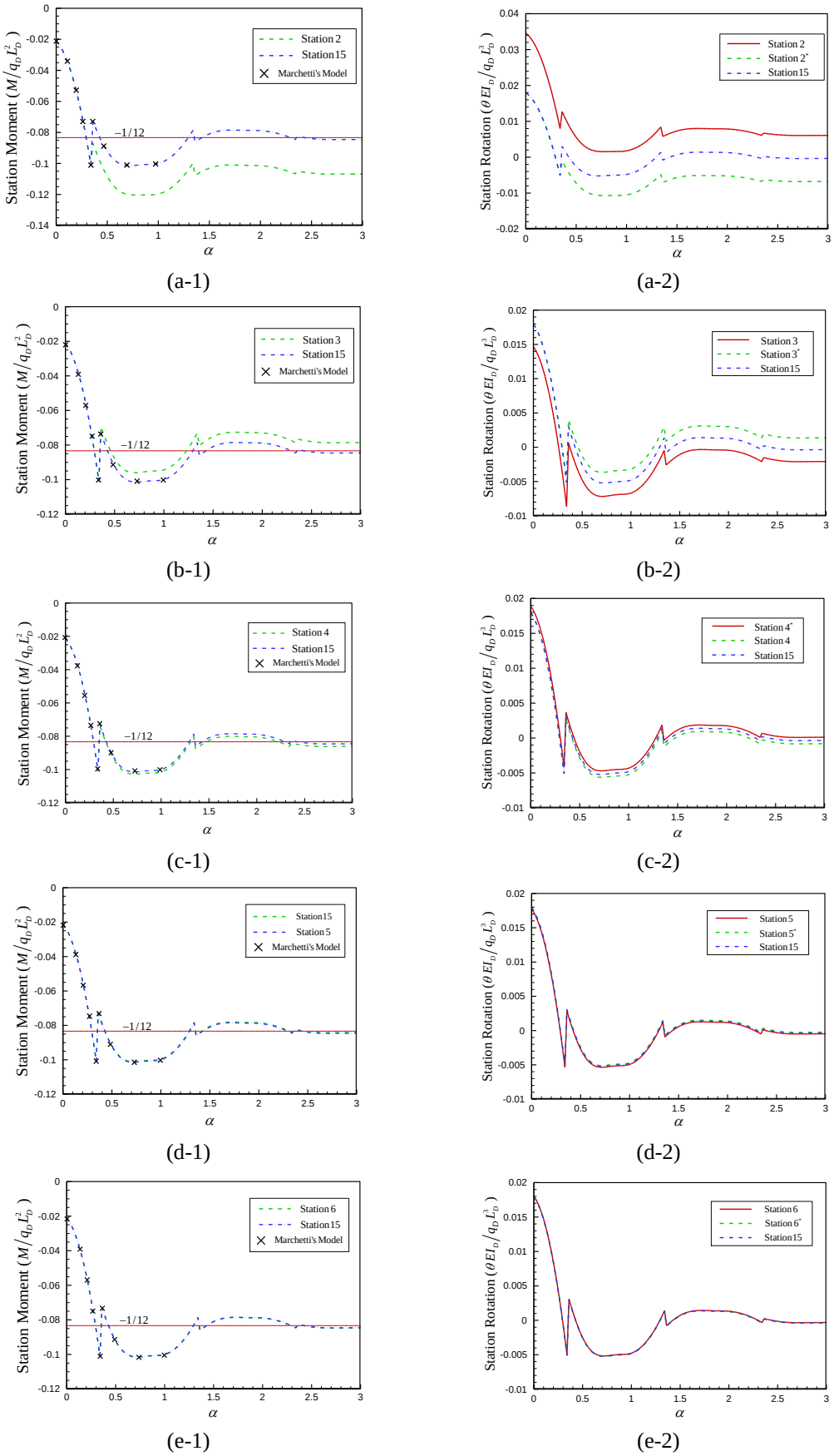

Fig. 11 Variations of moment and rotation for stations 2 to 6

[DOI: 10.22068/IJCE.13.1.112]

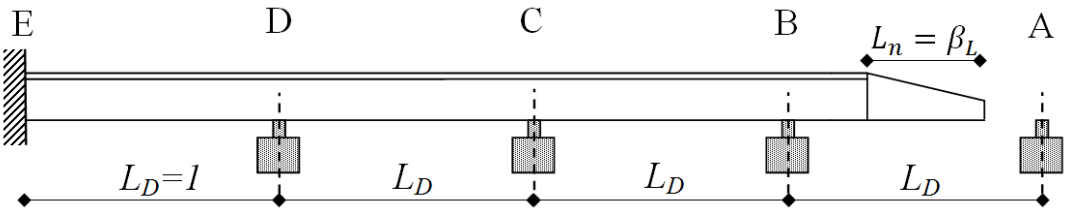

Fig. 12 The semi infinite beam model

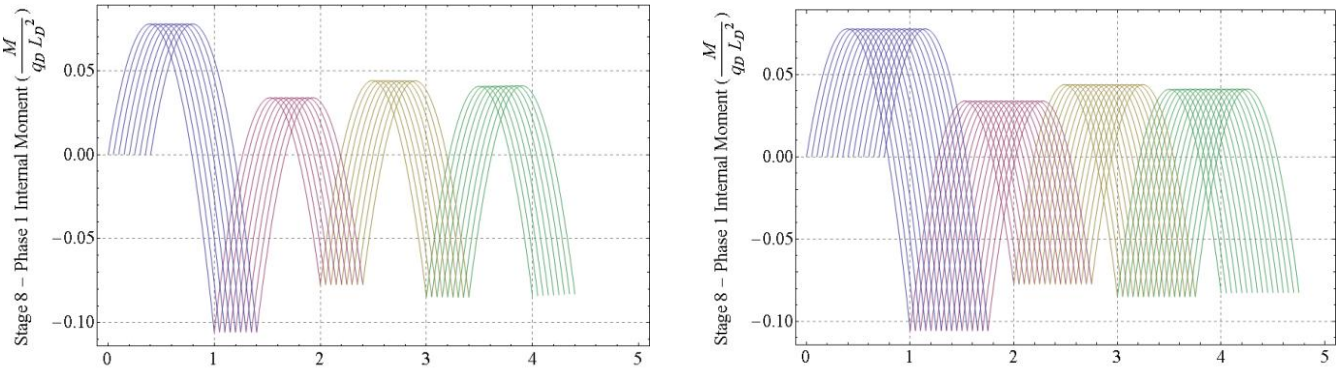

Fig. 13 Scenario of internal bending moment of eighth stage; a) phase 1, b) phase 2

Table 1 Appropriate values of a_1 and a_2 for different values of β_1 and β_0

β_1		1			0.9			**0.85**			0.8		
β_0		0	0.5	0.75	0	0.5	0.75	0	**0.5**	0.75	0	0.5	0.75
St.2	a_1	0.3325	0.3337	0.3334	0.3	0.3	0.3	0.2834	**0.2833**	0.2834	0.2667	0.2666	0.2667
	a_2	0.0416	0.0396	0.037	0.0304	0.0285	0.0262	0.0256	**0.0238**	0.0216	0.0213	0.0197	0.0176
St.3	a_1	0.2916	0.2917	0.2917	0.2895	0.2895	0.2895	0.2883	**0.2883**	0.2883	0.287	0.287	0.287
	a_2	0.0208	0.0214	0.022	0.0227	0.0232	0.0238	0.0235	**0.024**	0.0246	0.0242	0.0246	0.0252

6. Study on the Initial Stages of Launching

Moments of some stations in the initial stages of launching are more critical than farther stations. The problem lies in the fact that the bridge has not reached to its infinite continuous scheme yet. In this section the issue is discussed and some solutions are presented to reduce these station moments. To overcome the problem of critical conditions in the initial stages of launching, two main solutions are suggested:

1. Keeping some segments of the deck on the construction platform during launching of the initial stages. Generally, in practical projects a piece of superstructure, over half size of a mid span (one deck segment), is kept on the platform for each stage of launching.

2. Increasing bending stiffness of second station by shortening the length of the first span.

As will be concluded later, not only does second solution reduce temporary construction tensions but also it is suitable to optimize the static behavior of the bridge after construction in service time.

Fig. 13 shows the scenario of internal bending moment of superstructure parts during launching of phases one and two of eighth stage as an example. Moments are just shown for first four spans. Temperature effects, support settlements, shear deformation and platform loads are neglected and all spans are considered to be identical. Bridge spans act like fixed ends beams and moment at their supports and midpoints are approximately –1/12 and +1/24, respectively, except for some initial spans. This matter agrees with the results obtained in the previous sections.

In construction process, first span posses the maximum positive and negative bending moment (Fig. 13). By reducing length of the first span appropriately, maximum positive and negative moments of the first span can be reduced to be closer to that of other spans.

A numerical study is done for station two in the second stage and also for station three in the third stage of launching (Table. 1). In this table, values of a_1 and a_2 (Defined by equation (14)) for different values of β_1 and β_0 are given. The presented coefficients can be replaced in equation (14) to modify it for the initial stations. The bolded values of β_1 and β_0 ($\beta_1 = 0.85$ and $\beta_0 = 0.5$) are suitable to make initial stations behavior close to farther ones; because a_1 and a_2 are nearly equal to the values given by equation (14). It should be noted that a_1

[DOI: 10.22068/IJCE.13.1.112]

and a_2 are completely independent of geometrical and mechanical specifications of the nose.

Fig. 14 illustrates moment variation of station 2 in the second stage of launching with optimum values of β_1 and β_0 versus its moment variation with β_1 and β_0 as 1 and 0, respectively. This figure indicates that by choosing optimum values for β_1 and β_0, the moment variation of station 2 in second stage of launching completely conforms to the moment variation of station 15 in fifteenth stage.

Fig. 15 shows internal moment diagram of deck in an instant for launching of eighth stage (when nose tip distance from the first pier is 9.5 in normalized format) for β_1 equal to 1 and 0.85. Again, moments are just shown for first four spans. It can be concluded that not only does choosing optimum values for β_1 and β_0 optimize the launching moment of initial stations in their launching stages but also balances moment of different stations during all the stages of launching.

Similar moment diagram can be obtained when launching of bridge will be finished and the construction platform will be removed ($\beta_0 = 0$); moment diagram of this position resembles that of service time. Therefore, it can be concluded that the suggested value for β_1 can optimize the static performance of bridge in service time, as well.

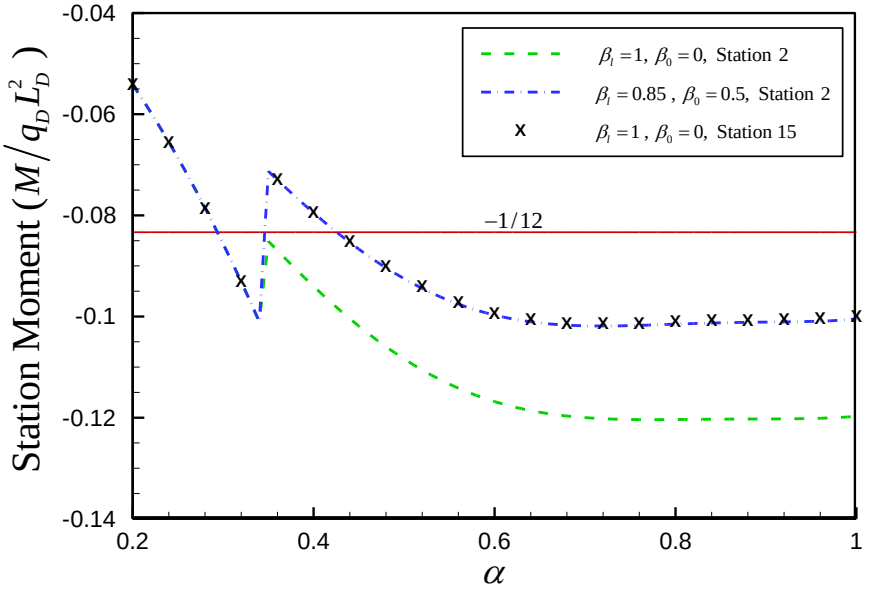

Fig. 14 Moment variation of the second station in second stage of launching with optimum values of β_1 and β_0

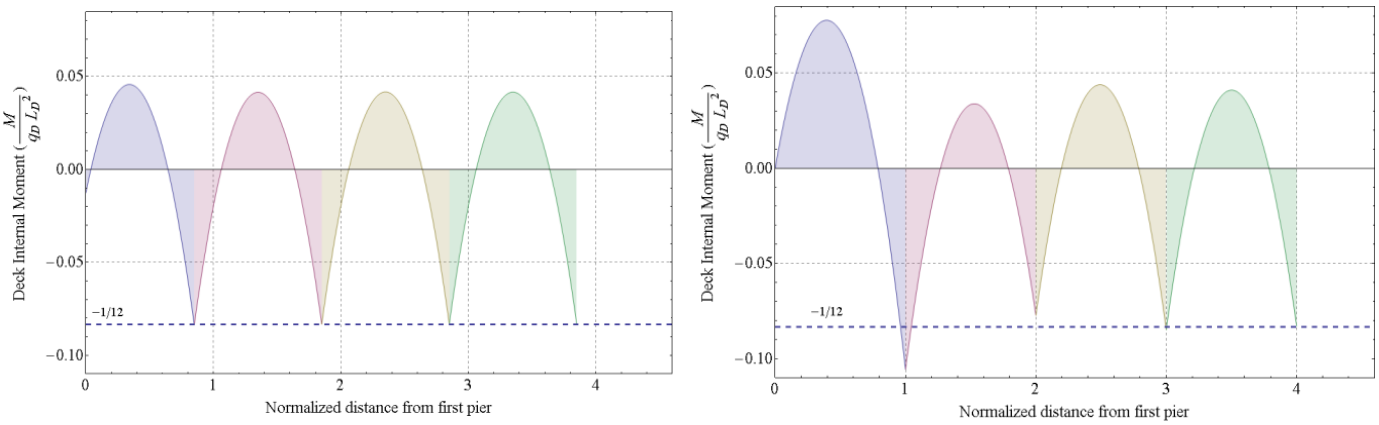

(a) (b)

Fig. 15 Moment diagram of deck in eighth stage; a) β_1=0.85, b) β_1=1

[DOI: 10.22068/IJCE.13.1.112]

7. Optimum Design of Nose Girder

This section leads to a comprehensive study on the developed semi infinite beam model. It should be noted that the main point to introduce the semi infinite beam model is its efficiency for parametric study on the nose-deck interaction through a simple structure with lower degrees of indeterminacy. It is intuitively obvious that the beam model, shown in Fig. 12, can be analyzed symbolically through different structural analysis techniques such as the theory of virtual work or the slope deflection method. In the previous section some remedies were suggested to preserve the advantages of a designed nose for all spans of launching. All in all, to give more insight into the realm of nose girder optimization, this developed simple model is applied along with considering a simple feasible directions method technique for optimization [18]. For the sake of brevity and simplicity, only absolute values of negative bending moment are taken in to account.

The foremost optimality criterion is that the nose-deck system performs optimal provided that the maximum bending moments at support B in the first and second phases of launching are equated as much as possible. Let M_{B1} and M_{B2} stand for the bending moment of support B in phase 1 and 2 of launching, respectively. Some required functions as f_1, f_2 and f are defined as follow:

$$f_1 = M_{B1}(1-\beta_L), \quad f_2 = \text{Max}(M_{B2}), \quad f = (f_1 - f_2)^2 \tag{15}$$

Likewise, the optimization problem regarding this optimality criterion can be stated as:

$$\begin{aligned} &\text{Find:} && \alpha, \beta_L, \beta_q, \beta_{EI} \\ &\text{Minimize:} && f \\ &\text{Subjected to:} && 1\text{-}\beta_L \le \alpha \le 1, \quad 0 \le \beta_L, \beta_q, \beta_{EI} \le 1 \end{aligned} \tag{16}$$

It is obvious that this problem may have many solutions as there are many combinations for β_L, β_q and β_{EI} to satisfy the equality for maximum moment of B in the both phases of launching. However, the problem can be constrained based on the qualitative studies given in Section 4. In this sense, by choosing a proper value for relative stiffness of the nose girder, $\beta_{EI} \ge 0.2$, maximum bending moment of support B will take place at $\alpha = 1$ (end of phase 2). The value of this maximum moment is independent of β_{EI} that is denoted by M_B^{EoL} (i.e., end of launch moment). Therefore, f_2 can be rewritten as:

$$f_2 = \text{Max}(M_{B2}) \cong M_B^{EoL} \tag{17}$$

In the other words, by focusing on $\alpha = 1$ position, β_{EI} can be eliminated from the unknown variables and thus for an arbitrary value of β_q, optimal values of β_L can be obtained by solving the following problem:

$$\begin{aligned} &\text{Find:} && \beta_L \\ &\text{Minimize:} && f \\ &\text{Subjected to:} && 0 \le \beta_L \le 1, \quad \beta_q^{opt} = \text{predetermined} \end{aligned} \tag{18}$$

It should be remarked here that in general the values of β_{EI} are interrelated with values of β_q; therefore, they must be chosen appropriately (See reference [2]). Nevertheless, in this section two different sets of values are assumed to make the solution procedure feasible; these values are rather close to that are used by the designers in the majority of practical projects. Now by considering $\beta_{EI} = 0.25$ and $\beta_q = 0.1$, the following results are obtained:

$$\begin{aligned} &\beta_L^{opt} = 0.667, \quad f_1, f_2 \to 0.0998, \\ &f \to 0.673E-14 \cong 0 \\ &\text{Max}(M_C) \to 0.0997 \end{aligned} \tag{19}$$

where, M_C stands for the moment of support C. Again by considering $\beta_{EI} = 0.3$ and $\beta_q = 0.15$ the following results are obtained:

$$\begin{aligned} &\beta_L^{opt} = 0.793, \quad f_1, f_2 \to 0.0931, \\ &f \to 0.4735E-14 \cong 0 \\ &\text{Max}(M_C) \to 0.0930 \end{aligned} \tag{20}$$

It is worth noting that in both of these cases, the maximum bending moment at support C is smaller than f_1 and f_2. As can be seen, using the simple semi infinite beam model makes a good platform for optimal design of the nose girder.

The moment variation of support B, as in Fig. 12, through the FE model, based on the obtained values for nose specifications in (19) and (20) and that well-known values introduced in Section 4, are shown in Fig. 16. Moreover, for the sake of verification, the results of RTM method developed in [9], for $\beta_{EI} = 0.3$, $\beta_q = 0.15$ and $\beta_L = 0.793$, are shown in this figure. It should be pointed out that all the spans are assumed to be identical, and effects of support settlement, shear deformation and platform load are neglected.

[DOI: 10.22068/IJCE.13.1.112]

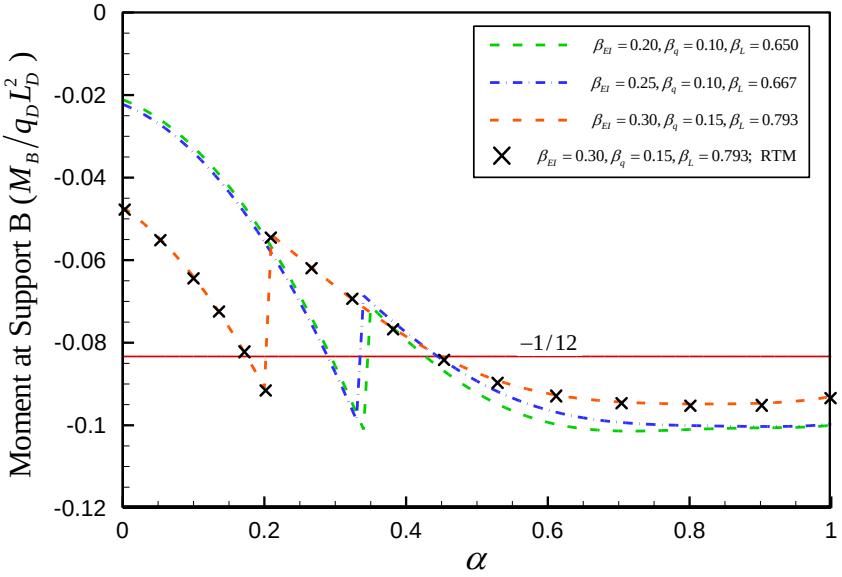

Fig. 16 Moment variation of support B for the optimum values of nose specifications

8. Conclusion

In this paper, a new finite element model has been developed to analyze the construction stages of incrementally launched bridges. This model eliminates many limitations of some previous models and can be used for studying on behavior of the bridge considering different load cases. Effects of support settlement, shear strain, temperature gradient, construction platform and unequal spans can be considered in the presented model. By using a simple technique, all parameters involved in the problem can be normalized with respect to main specifications of deck, and all unknown variables are obtained as dimensionless normalized quantities. This method is especially advantageous for studying on the nose-deck interaction and optimizing the nose specifications.

A brief study on the nose-deck interaction and optimum specifications regarding the effect of temperature gradient and shear strain has been done. The final results indicate that the effects of these two parameters on the nose-deck interaction are not generally significant.

By using the presented FE model, an extensive study has been done to assess the accuracy of the Marchetti's conventional model. It has been concluded that this model is only accurate when there are at least five spans behind the under study station which means that the simplified model is not useful for studying on initial stages of launching. Therefore, a comprehensive study is conducted regarding rotations of pier sections during launching. Such a study results in some modification factors through which the Marchetti's formulation can be modified for initial stages of launching easily. Moreover, a new simple semi infinite beam model has risen out of this study. It has been demonstrated that the model can be useful for optimum design of the nose girder parameters and also efficient for parametric study of the nose-deck system.

In the FE model the effects of first span length and length of platform segments are considered, as well. It has been shown that the first span length plays a very important role for resolving the critical conditions of the initial stages. Therefore, suitable ranges for these parameters, in the view of optimum static performance of bridge after launching, are introduced. By using these optimal values, the initial stations act like the farther ones; in addition, the benefits of using a well-optimized nose girder can be preserved for all the constructional stages.

References

[1] Störfix. Website of the Wikimedia commons. [Online] http://commons.wikimedia.org/wiki/File:Truckenthalbruecke-Juni2010-2.jpg, 2010.

[2] Rosignoli M. Bridge Launching, Thomas Telford, London, 2002.

[3] Marzouk M, El-Dein HZ, El-Said M. Application of computer simulation to construction of incremental launching bridges, Journal of Civil Engineering and Management, 2007, No. 1, Vol. 13, pp. 27-36.

[4] Rosignoli M. Nose-deck interaction in launched prestressed concrete bridges, Journal of Bridge Engineering, 1998, No. 1, Vol. 3, pp. 21-27.

[5] Zellner W, Svensson H. Incremental launching of structures, Journal of Structural Engineering, 1983, No. 2, Vol. 109, pp. 520-37.

[6] AASHTO, Bridge construction practices using incremental launching, Highway Subcommittee on Bridges and Structures, 2007.

[7] Marchetti ME. Specific design problems to bridges built using the incremental launching method, Journal of Structural Engineering, 1984, No. 3, Vol. 6, pp. 185-210.

[8] Fontan AN, Diaz JM, Baldomir A, Hernandez S. Improved optimization formulations for launching nose of incrementally launched prestressed concrete bridges, Journal of Bridge Engineering, 2011, No. 3, Vol. 16, pp. 461-470.

[9] Rosignoli M. Reduces-transfer-matrix method for analysis of launched bridges, Structural Journal, 1999, No. 4, Vol. 96, 603–608.

[DOI: 10.22068/IJCE.13.1.112]

[10] Sasmal S, Ramanjaneluyu K, Srinivas V, Gopalakrishnan S. Simplified computational methodology for analysis and studies on behavior of incrementally launched continuous bridges, Structural Engineering & Mechanics, 2004, No. 2, Vol. 17, pp. 245-266.

[11] Sasmal S, Ramanjaneluyu K. Transfer matrix method for construction phase analysis of incrementally launched prestressed concrete bridges, Engineering Structures, 2006, No. 13, Vol. 28, pp. 1897-1910.

[12] Arici M, Granata MF. Analysis of curved incrementally launched box concrete bridges using the transfer matrix method, Journal of Bridge Engineering, 2007, Nos. 3-4, Vol. 3, pp. 165–181.

[13] Jung K, Kim K, Sim CW, Jay Kim JH. Verification of incremental launching construction safety for the ilsun bridge, the world's longest and widest prestressed concrete box girder with corrugated steel web section, Journal of Bridge Engineering, 2011, No. 3, Vol. 16, pp. 453-460.

[14] Lee HW, Ahn TW, Kim KY. Nose-deck interaction in ilm bridge proceeding with tapered sectional launching nose, Computational Mechanics, Beijing, China, 2004.

[15] Nie JG, Cai CS. Steel–concrete composite beams considering shear slip effects, Journal of Structural Engineering, 2003, No. 4, Vol. 129, pp. 495-506.

[16] Nie JG, Cai CS, Zhou TR, Li Y. Experimental and analytical study of prestressed steel–concrete composite beams considering slip effect, Journal of Structural Engineering, 2007, No. 4, Vol. 133, pp. 530-540.

[17] Sennah K, Kennedy JB, Nour S. Design for shear in curved composite multiple steel box girder bridges, Journal of Bridge Engineering, 2003, No. 3, Vol. 8, pp. 144-152.

[18] Vanderplaats GN. Numerical Optimization Techniques for Engineering Design: with Applications, McGraw-Hill New York, 1984.

[DOI: 10.22068/IJCE.13.1.112]